IEEE Photonics Journal
An IEEE Photonics Society Publication

Open Access

Deeply Etched Inner-Cavity Pit Reflector

Volume 9, Number 1, February 2017

M. Dernaika
L. Caro
N. P. Kelly
J. K. Alexander
F. Dubois
P. E. Morrissey
F. H. Peters

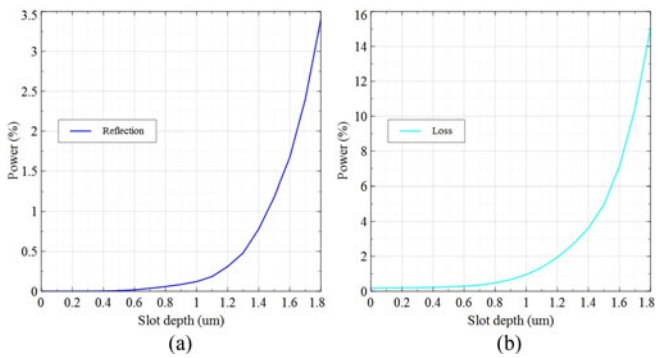

DOI: 10.1109/JPHOT.2017.2656252
1943-0655 © 2017 IEEE

IEEE photonics SOCIETY

IEEE

Deeply Etched Inner-Cavity Pit Reflector

M. Dernaika,[1,2] L. Caro,[1,3] N. P. Kelly,[1,3] J. K. Alexander,[1,3] F. Dubois,[1,3] P. E. Morrissey,[1,4] and F. H. Peters[1,3]

[1]Integrated Photonics Group, Tyndall National Institute, Cork T12 R5CP, Ireland
[2]Department of Electrical and Electronic Engineering, University College Cork, Cork, Ireland
[3]Department of Physics, University College Cork, Cork, Ireland
[4]Photonics Packaging Group, Tyndall National Institute, Cork T12 R5CP, Ireland

DOI:10.1109/JPHOT.2017.2656252

Manuscript received December 11, 2016; revised January 17, 2017; accepted January 18, 2017. Date of publication January 20, 2017; date of current version February 9, 2017. This work was supported by the Science Foundation Ireland under Grant SFI 13/IA/1960 and Grant 12/RC/2276 (I-PIC). Corresponding author: M. Dernaika (e-mail: mohamad.dernaika@tyndall.ie).

Abstract: A deeply etched pit reflector is presented in this paper. The pit is not depth sensitive and has a comparable reflection and loss to a slot. Moreover, a two-section 750 μm laser cavity based on the pits is demonstrated. The laser achieved a side-mode suppression ratio of 40 dB, a linewidth of 280 KHz, and tuning across 40 nm.

Index Terms: Semiconductor lasers, laser tuning, optical waveguides.

1. Introduction

Regrowth-free semiconductor single mode lasers that employ standard ultraviolet lithography for patterning have drawn considerable interest due to their potential to lower the overall cost of photonics components. They offer a much simpler fabrication approach than distributed feedback (DFB) and distributed Bragg reflector (DBR) lasers by eliminating the need of high resolution lithography and epitaxial regrowth, which is costly and time consuming.

An example of such lasers, that are also suitable for integration and advanced modulation formats are the slotted Fabry Perot (SFP) lasers [1]–[3]. Slots introduce index perturbation along the ridge, which leads to small reflections. The reflections create sub-cavities, that result in mode selectivity based on the coupled resonance of various cavities [4]–[6]. SFP lasers exhibit high side mode suppression ratio (SMSR), wide tuning range and narrow linewidth [7]–[9]. They also have been employed in single facet and facet-less laser configurations that allows monolithic integration of the laser with other devices such as modulators and photodiodes [10]–[12].

A limitation of the slot is that the reflection, loss, and transmission of the slot are exponentially dependent on the slot depth, whereas slot width has little effect [5], [13]. Achieving the same slot depth at each fabrication run, or in certain cases across the same chip is not always attainable using plasma etching. Moreover, due to the high sensitivity to depth, inconsistency in a laser's performance can occur across a wafer. To demonstrate the sensitivity of the slot etch depth, a simulation module consisting of a cavity with single slot was developed using ModePROP from Rsoft. The aforementioned software employs the Eigen mode expansion method, (EEM) an omnidirectional technique that take all reflections into account [14]–[16]. The simulation plots are shown in Fig. 1.

The plot in Fig. 1 displays reflection and loss as a function of a slot depth with a ridge height of 1.8 μm. Fig. 1(a) shows the rapid increase of the reflection with varying slot depth, where a slight depth difference as small as 50-100 nm can have a significant effect on the reflection.

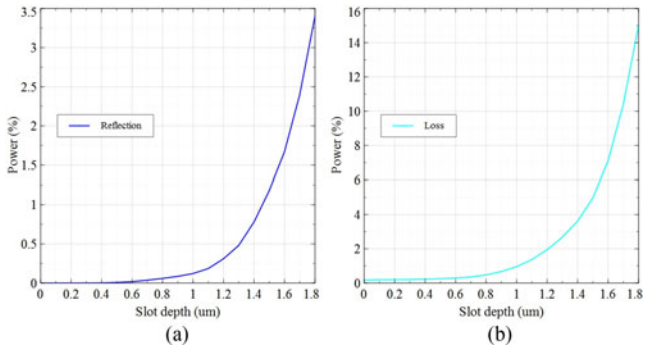

Fig. 1. Simulation module of slot showing depth effect on (a) reflection and (b) loss.

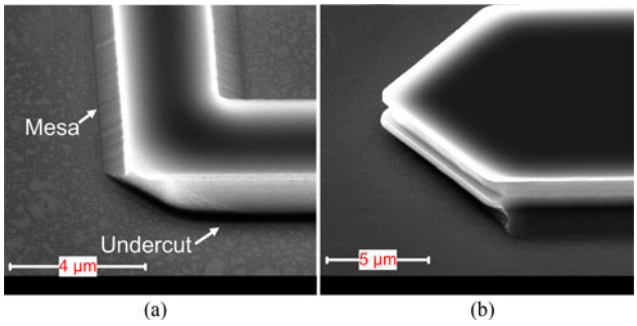

Fig. 2. (a) Effect of wet etch on two ridges with different orientation. (b) Non-uniform layer etching.

Fig. 1(b) shows the loss curve as a function of the etch depth. The loss power is much higher than the reflected power due to scattering losses introduced by the slot, which agrees well with both analytical model presented in [13] and experimental data [6].

However, this issue can be addressed by adding an etch stop layer just above the active region and using wet etch in combination with the dry etch [17], [18]. Although, this method will ensure a consistent depth across the chip with various fabrication runs, it will add complexity to the fabrication process, and restrict the cavity designs on the chip due to the influence of crystal orientation on chemical etching of InP [19]–[23]. The wet etch effects can be seen in Fig. 2 SEM images. Fig. 2(a) show how the etch outcome can be different for two ridges with various orientations, and Fig. 2(b) shows another situation where the chemical etchant creates a non-uniform layer etch pattern.

In this paper, we demonstrate a pit reflector in a form of a hole in the waveguide that operates similarly to the slot. However, the pit is not depth sensitive because it is deeply etched through the active region. By eliminating the need to the wet etch, the chip can accommodate devices with different orientations and the device yield is also expected to increase. In addition, due to its intrinsic design the pit is compatible with high index contrast ridge waveguides structures [24], [25]. Moreover, the process does not require the use of Focused Ion beam etching (FIBE) to create the pits, or a complicated setup as previously reported in [26]. In the next section the fabrication process of the pit will be presented along with the pit characterization and comparison with the slots. In the last section, a 2-section laser that uses 4 pits as a reflector, will be presented to demonstrate that the pits can be efficiently used as a single mode selector. This 750 μm long laser exhibits a 40 dB SMSR with a linewidth of 280 kHz and tuning range across 40 nm.

2. Fabrication and Characterization

The deeply etched pit is fabricated using a self-aligned process. The ridge and the pit are defined in the same lithography layer; an SEM image of the pit, is shown in Fig. 3.

Fig. 3 shows a post-fabrication SEM of the 1 μm wide and 1.5 μm long pit with ridge oxide opening and deposited metal. the rectangle shape surrounding the pit, and the ridge is the deep

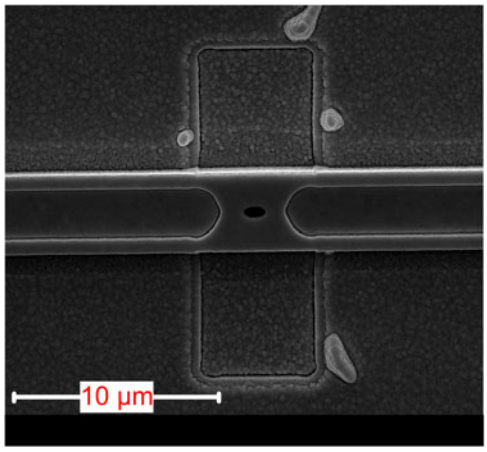

Fig. 3. SEM image of the Pit reflector.

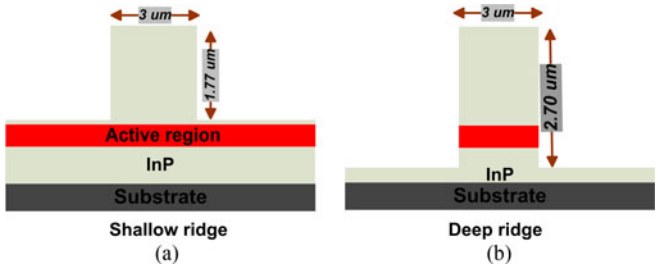

Fig. 4. (a) Shallow ridge. (b) Deeply etched ridge.

etch region which is defined in another lithography layer. The epitaxial wafer used in the fabrication is commercially available IQE material. It comprises 5 $\times$ 6 nm AlInGaAs strained quantum wells sandwiched between 6 $\times$ 10 nm barriers, the total thickness of the active region is 400 nm. A 20 nm GaInAsP etch stop layer is grown on top of the active region and under a 1580 nm InP layer. The metal contact layers consist of 50 nm GaInAsP and 200 nm highly doped GaInAs. The deposited p-metal was 20:350 nm Ti: Au and the n-metal was 20:250 nm Ti: Au. The fabrication process consisted of 4 lithography layers; one layer is used to define the ridge and the pit, and the other three layers are utilized for the deep etch region, oxide opening, and metal lift-off, respectively. The process comprises of two etch depths, shallow for the ridge and deep for the pit reflector. The two depth are illustrated in Fig. 4

The shallow ridge height is 1.77 μm, and the deep region is 2.7 μm; both shallow and deep ridges have a width of 3 μm. Fig. 5 shows a cross-section SEM image of the pit obtained by using FIBE, to ensure that the pit has a fixed width with the ridge height. After the semiconductor etch, the pit is filled with 400 nm silicon oxide that is used as a passivation layer.

To assess the performance of the pit reflector in comparison with a slot, two 1.1 mm long Fabry Perot cavities were fabricated, one cavity having a slot and another with a pit. Both reflectors were placed 200 μm from the first cleaved facet and 900 μm from the second cleaved facet. The Light-Intensity (L-I) curve of both structures is shown in Fig. 6

The light was coupled using a lensed fiber while sweeping the current from 0 mA to 100 mA. The pit (red line) and slot (blue line). both lase at around 31 mA with almost identical slope efficiency. The spectrum taken at the lasing threshold for both cavities can be seen in Fig. 7.

The localized reflections from the slot and pit cause a periodic modulation of the optical spectra. The modulation effect on the gain envelope can be clearly seen in Fig. 7. Both structures have a comparable spectral behavior, and modulation depth, which suggests that the reflection of both

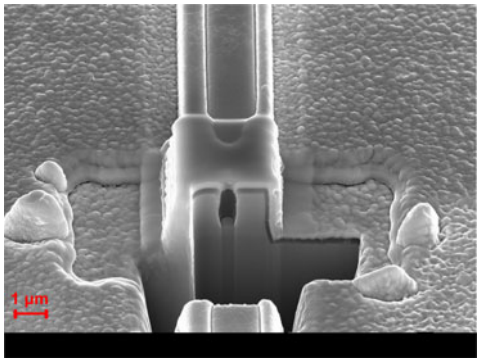

Fig. 5. Pit cross section obtained using FIBE.

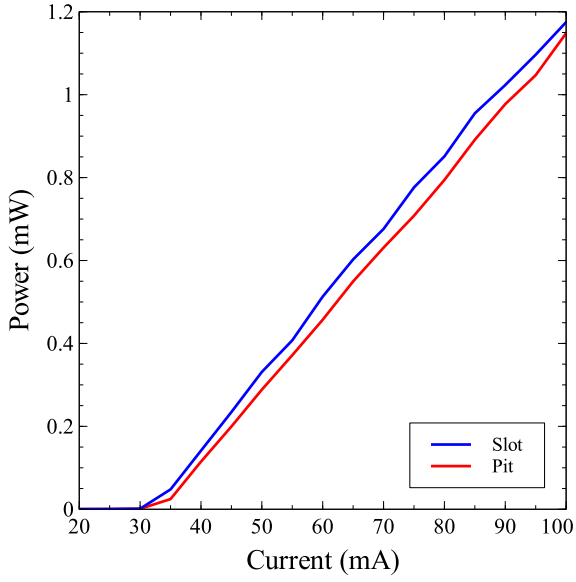

Fig. 6. L-I curve of two cavities with pit (red line) and slot (blue line).

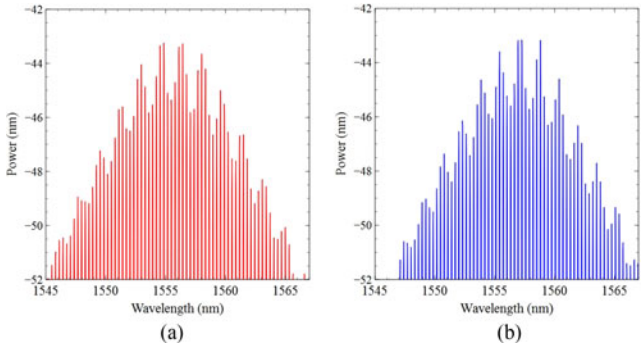

Fig. 7. Optical spectrum (a) cavity with a pit and (b) cavity with a slot.

structures is also comparable. In order to confirm that the reflections were caused by the pits and not by the rectangle deep/shallow waveguide transitions, lasers were made without pits, but with identical rectangle deep/shallow transitions, and no measurable reflections or periodic modulation were seen using the spectral analysis.

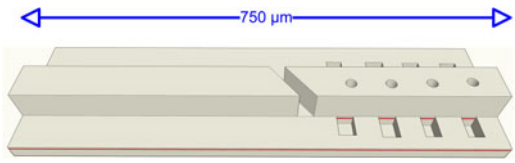

Fig. 8. Laser cavity with four deeply etched pits.

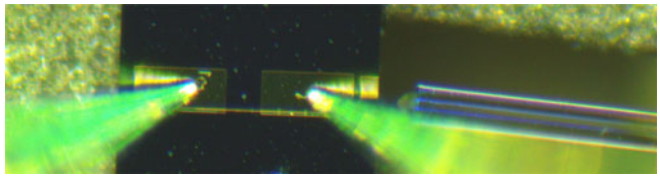

Fig. 9. Microscope image of the device under test.

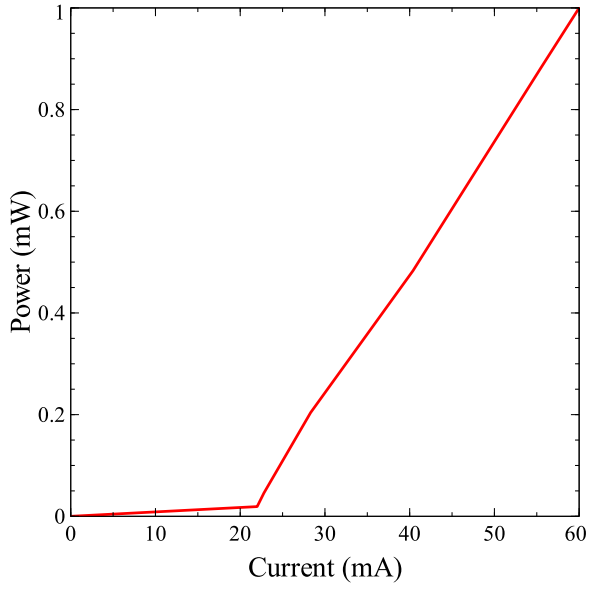

Fig. 10. L-I curve of the DUT.

3. Results and Discussion

A two section laser cavity that comprises four pits was fabricated to demonstrate that the deeply Pit etched reflectors works well as a single mode laser. The cavity design is shown in Fig. 8.

Fig. 8 show the two section laser with a total length of 750 μm and 4 pits with a spacing of 70 μm. A 7 degrees angled slot is used to provide electrical isolation between the two sections. The mirror section is 350 μm long and consists of four pits, and the gain section is 400 μm long.

The microscope image in Fig. 9 shows the device under test (DUT). Two probes were used to inject current into the individual sections. The optical feedback is provided from the Air/semiconductor interface from the two uncoated cleaved facets. Therefore a lensed fiber was employed to collect the light from the right facet as shown in Fig. 9. The laser was mounted on a temperature controlled brass chuck to ensure thermal stability of the DUT with varying current injection, the temperature of the chuck was fixed at 20 degrees Celsius.

Fig. 10 shows the laser L-I curve obtained by biasing the gain section at 10 mA and sweeping the mirror section from 0 mA to 100 mA. Introducing four pits into the cavity increased the lasing threshold by few milliamps in comparison with a device with no pits. Using a fast Fourier transform (FFT) algorithm it was possible to extract the resonating sub-cavities in the laser caused from the

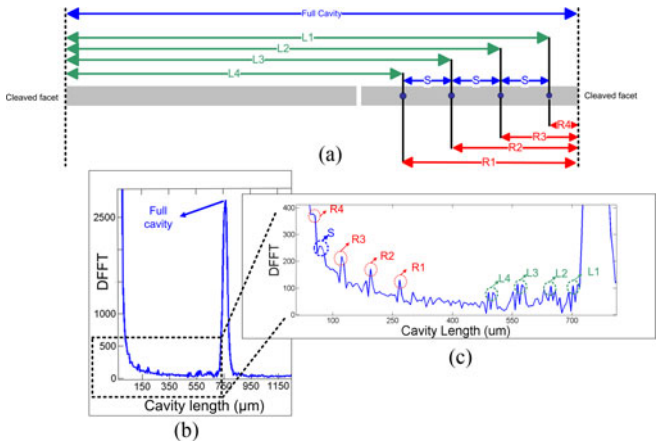

Fig. 11. (a) Cavity resonance map between the pits and cleaved facets. (b) FFT cavity analysis of the laser spectrum. (c) FFT zoom in showing Pits sub-cavities.

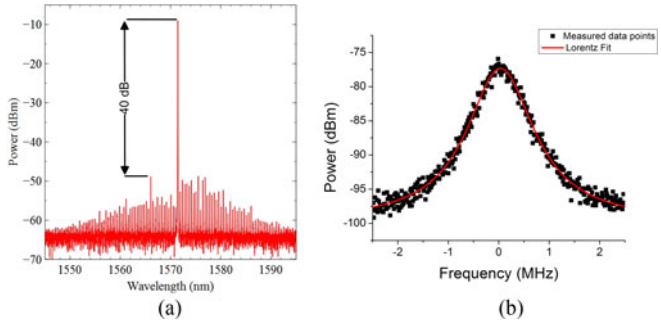

Fig. 12. (a) Laser single mode output with SMSR of 40 dB. (b) 280 kHz measured linewidth and lorentz fit.

pits. Fig. 11(a) shows the various resonances between the facets and pits, as well as the resonance between pits. The labels L1 to L4 represents the interaction of the left facets with the various pits and R1 to R4 corresponds the interaction of the pits with the right facet. In addition, the full cavity and inner pits spacing S is shown.

Fig. 11(b) shows the full FFT spectrum that shows a peak at 750 μm which corresponds to the spacing between the 2 facets. Fig. 11(c) is a close up figure of the FFT spectrum in the region where the pits interact with each facet as well as with each other. The labels in Fig. 11(c) correspond to the physical length of the sub-cavities shown in Fig. 11(a), clearly showing reflection from each of the individual pits leading to mode selectivity. The spectrum of the pit laser is shown in Fig. 12(a) with an SMSR of approximately 40 dB and output power $>$2 mW. Fig. 12(b) shows the 280 kHz laser linewidth, which is the full width at half maximum (FWHM) of the measured spectrum. the linewidth measured was obtained using a delayed self-heterodyne linewidth setup with 50 km fiber delay line in a recirculating loop configuration that has a resolution of $<$2 KHz [27].

The laser is tunable across 40 nm with an SMSR ranging from 30 dB to 40 dB that extend from 1540 nm to 1590 nm with a step of approximately 5 nm that correspond to the free spectral range (FSR) of 70 μm cavity that matches the spacing between the pits. Typically, the spacing between the reflectors dominate the tuning of such lasers [11]. The FSR of the mirrors dominate the mode hops of the laser cavity, as can be clearly seen in Fig. 13

Fig. 13 shows a sample of the tuning of the laser with 4 wavelength with a step of $\Delta\lambda$ which is $\approx$ 5 nm corresponding to the pit mirrors FSR. In this example, by increasing the total injected current from 80 mA to 150 mA the laser is tuned while maintaining an SMSR between 30 and 40 dB across all wavelengths.

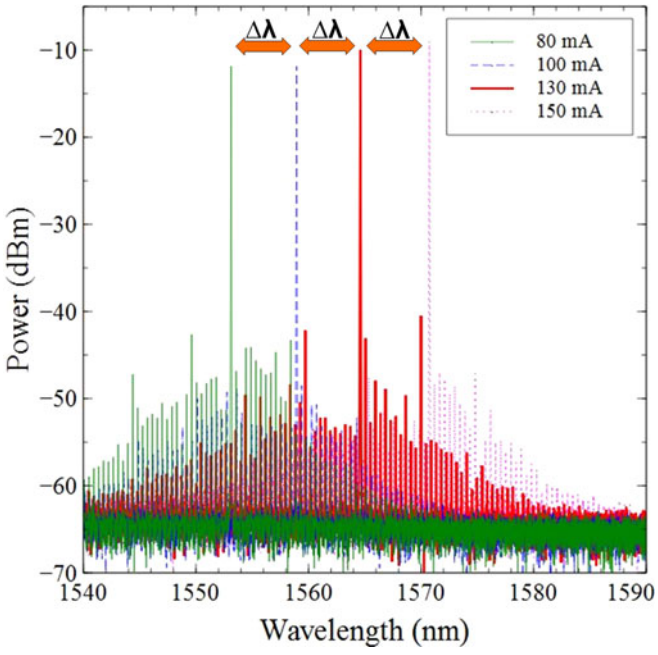

Fig. 13. Single mode tuning with relevant injected current.

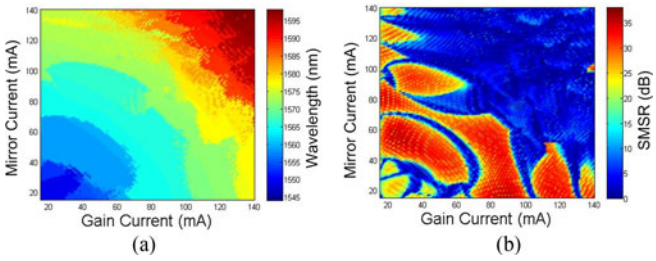

Fig. 14. Color tuning map of (a) wavelength in function gain and mirror current. (b) SMSR in function of gain and mirror current.

The full tuning map for the pit laser with the corresponding mirror and gain current is shown in Fig. 14

The color map in Fig. 14(a) shows the wavelength region in function of the varying current in the mirror section and the gain section, whereas Fig. 14(b) shows SMSR value in function of the gain and the mirror section. The red areas show the region where the SMSR is $>$30 dB, and the blue region is where the laser is mostly multimode. As shown in Fig. 14, the laser can achieve an SMSR between 30 dB and 40 dB for wavelengths extending over more than 40 nm tuning range.

4. Conclusion

This paper reports a single mode laser based on a deeply etched pit reflector that does not require chemical wet etching. A comparison between an etched slot and the pit showed a similar power and spectral behavior derived from the L-I curve and optical spectrum of two cavities comprising the slot and pit. Moreover, a 750 μm two section laser was fabricated to demonstrated the efficiency of the pits as a single mode selector. The laser comprised four pits and achieved an SMSR of 40 dB and a linewidth of 280 kHz. The laser tuning range extends over 40 nm with an SMSR up to 40 dB.

References

[1] C. Herbert *et al.*, "Discrete mode lasers for communication applications," *IET Optoelectron.*, vol. 3, no. 1, pp. 1–17, 2009.
[2] Y. Zhang *et al.*, "A hybrid silicon single mode laser with a slotted feedback structure," *Opt. Exp.*, vol. 21, no. 1, pp. 877–883, 2013.
[3] Y. Zhang, H. Wang, H. Qu, S. Zhang, and W. Zheng, "Slotted hybrid iii–v/silicon single-mode laser," *IEEE Photon. Technol. Lett.*, vol. 25, no. 7, pp. 655–658, Apr. 2013.
[4] S. O'Brien *et al.*, "Design, characterization, and applications of index-patterned fabry–pérot lasers," *IEEE J. Sel. Topics Quantum Electron.*, vol. 17, no. 6, pp. 1621–1631, Nov./Dec. 2011.
[5] Q. Lu, W.-H. Guo, D. Byrne, and J. F. Donegan, "Design of slotted single-mode lasers suitable for photonic integration," *IEEE Photon. Technol. Lett.*, vol. 22, no. 11, pp. 787–789, Jun. 2010.
[6] B. Corbett, C. Percival, and P. Lambkin, "Multiwavelength array of single-frequency stabilized fabry-perot lasers," *IEEE J. Quantum Electron.*, vol. 41, no. 4, pp. 490–494, 2005.
[7] D. Byrne, J. Donegan, Q. Lu, and W. Guo, *A Tunable Semiconductor Lased Based on Etched Slots Suitable for Monolithic Integration*. Rijeka, Croatia: INTECH Open Access, 2010.
[8] B. Kelly *et al.*, "Discrete mode laser diodes with very narrow linewidth emission," *Electron. Lett.*, vol. 43, no. 23, 2007.
[9] K. Shi *et al.*, "Characterization of a tunable three-section slotted fabry–perot laser for advanced modulation format optical transmission," *Opt. Commun.*, vol. 284, no. 6, pp. 1616–1621, 2011.
[10] Q. Lu *et al.*, "Single mode lasers based on slots suitable for photonic integration," *Opt. Exp.*, vol. 19, no. 26, pp. B140–B145, 2011.
[11] D. C. Byrne *et al.*, "Discretely tunable semiconductor lasers suitable for photonic integration," *IEEE J. Sel. Topics Quantum Electron.*, vol. 15, no. 3, pp. 482–487, May/Jun. 2009.
[12] J. Engelstaedter, B. Roycroft, and B. Corbett, "Laser and detector using integrated reflector for photonic integration," *Electron. Lett.*, vol. 44, no. 17, pp. 1017–1019, 2008.
[13] Q. Lu *et al.*, "Analysis of slot characteristics in slotted single-mode semiconductor lasers using the 2-d scattering matrix method," *IEEE Photonics Technol. Lett.*, vol. 18, no. 24, pp. 2605–2607, 2006.
[14] S. Schelkunoff, "Generalized telegraphist's equations for waveguides," *Bell Syst. Techn. J.*, vol. 31, no. 4, pp. 784–801, 1952.
[15] D. Marcuse, *Theory of Dielectric Optical Waveguides*. Amsterdam, The Netherlands: Elsevier, 2013.
[16] D. F. Gallagher and T. P. Felici, "Eigenmode expansion methods for simulation of optical propagation in photonics: Pros and cons," *Proc. SPIE*, vol. 4987, pp. 69–82, 2003.
[17] R. Phelan *et al.*, "A novel two-section tunable discrete mode fabry-perot laser exhibiting nanosecond wavelength switching," *IEEE J. Quantum Electron.*, vol. 44, no. 4, pp. 331–337, Apr. 2008.
[18] C. Guignard *et al.*, "Ultra-narrow (sub-mhz) linewidth emission from discrete mode laser diodes," in *Proc. Eur. Conf. Lasers Electro-Opt., 2007 Int. Quantum Electron. Conf.*, Munich, 2007, pp. 1–1.
[19] N. Siwak, X. Fan, and R. Ghodssi, "Fabrication challenges for indium phosphide microsystems," *J. Micromech. Microeng.*, vol. 25, no. 4, 2015, Art. ID 043001.
[20] D. Cuypers, S. De Gendt, S. Arnauts, K. Paulussen, and D. van Dorp, "Wet chemical etching of inp for cleaning applications i. an oxide formation/oxide dissolution model," *ECS J. Solid State Sci. Technol.*, vol. 2, no. 4, pp. P185–P189, 2013.
[21] J. J. Kelly and H. G. Philipsen, "Anisotropy in the wet-etching of semiconductors," *Curr. Opin. Solid State Mate. Sci.*, vol. 9, no. 1, pp. 84–90, 2005.
[22] S. Adachi and H. Kawaguchi, "Chemical etching characteristics of (001) inp," *J. Electrochem. Soc.*, vol. 128, no. 6, pp. 1342–1349, 1981.
[23] A. Stano, "Chemical etching characteristics of ingaas/inp and inalas/inp heterostructures," *J. Electrochem. Soc.*, vol. 134, no. 2, pp. 448–452, 1987.
[24] D. Liang, D. Hall, J. Y.-T. Huang, J.-Y. Yeh, and L. Mawst, "High-index-contrast oxide-confined gaasp/ingaasn multi-quantum-well ridge waveguide lasers," in *Proc. 2006 IEEE 20th Int. Semiconductor Laser Conf.*, 2006, pp. 165–166.
[25] C. Seibert and D. Hall, "High-index-contrast ridge waveguide laser with thermally oxidised etched facet and metal reflector," *Electron. Lett.*, vol. 46, no. 15, pp. 1077–1078, 2010.
[26] D. Kozlowski, J. Young, J. England, and R. Plumb, "Longitudinal mode control in 1.3 um Fabry-Perot lasers by mode suppression," *Proc. Inst. Elect. Eng. Optoelectron.*, vol. 143, no. 1, pp. 71–76, 1996.
[27] H. Tsuchida, "Simple technique for improving the resolution of the delayed self-heterodyne method," *Opt. Lett.*, vol. 15, no. 11, pp. 640–642, 1990.